Cancer Letters 317 (2012) 226–236

Contents lists available at SciVerse ScienceDirect

Cancer Letters

journal homepage: www.elsevier.com/locate/canlet

RXRα deletion and E6E7 oncogene expression are sufficient to induce cervical malignant lesions *in vivo*

Rodolfo Ocadiz-Delgado [a,b], Eduardo Castañeda-Saucedo [c,1], Arup K. Indra [c,g,2], Rogelio Hernandez-Pando [d], Pedro Flores-Guizar [a], Jose Luis Cruz-Colin [a], Felix Recillas-Targa [e], Guillermo Perez-Ishiwara [b], Luis Covarrubias [f], Patricio Gariglio [a,*]

[a] Dept. of Genetics & Molecular Biology, Centro de Investigacion y de Estudios Avanzados del IPN (CINVESTAV-IPN). Av. IPN 2508, Col. San Pedro Zacatenco, 07360. Mexico, DF, Mexico
[b] Molecular Biomedicine, PlBioM, Escuela Nacional de Medicina y Homeopatia-IPN. Guillermo Massieu Helguera 239 Fracc. La Escalera-Ticoman. Mexico, DF, Mexico
[c] Institut de Génétique et de Biologie Moléculaire et Cellulaire (IGBMC), Centre National de la Recherche Scientifique (CNRS), Institut National de la Santé et de la Recherche Médicale (INSERM), Université Louis Pasteur, Illkirch-Cedex, Strasbourg, France
[d] Dept. of Pathology, Instituto Nacional de Ciencias Medicas y Nutricion Salvador Zubiran (INCMNSZ). Vasco de Quiroga 15, Col. Seccion XVI, Tlalpan, 14000. Mexico, D.F., Mexico
[e] Departamento de Genética Molecular, Instituto de Fisiología Celular, Universidad Nacional Autónoma de México, Mexico
[f] Institute of Biotechnology, Universidad Nacional Autónoma de México, Mexico
[g] Department of Dermatology, Oregon Health and Science University, Portland, OR 97239, USA

ARTICLE INFO

Article history:
Received 13 July 2011
Received in revised form 23 November 2011
Accepted 23 November 2011

Keywords:
E6E7
HPV
Retinoid receptor
Cervical cancer
Murine models

ABSTRACT

Cervical cancer is the second leading cause of cancer deaths among women worldwide. High-Risk-Human Papillomaviruses (HR-HPVs) play an important etiologic role in the development of carcinoma of the uterine cervix. However, host factors are important in determining the outcome of genital HPV infection as most cervical precancerous lesions containing HR-HPVs do not progress to invasive carcinomas. Retinoids, acting through nuclear receptors (RARs, RXRs), play a crucial role in cervix development and homeostasis regulating growth and differentiation of a wide variety of cell types; indeed, they can inhibit cell proliferation, and induce cell differentiation or apoptotic cell death. Here we introduce a mouse model that develops spontaneously malignant cervical lesions allowing the study of the cooperative effect between HPV16E6E7 expression and the lack of RXRα in cervical cancer development. This model could be useful to study multistep carcinogenesis of uterine cervix tissue and might improve chemopreventive and chemotherapeutic strategies for this neoplasia.

1. Introduction

Cancer development commonly takes decades to arise, and follows a progressive histopathological pattern that involves acquisition of multiple genetic and epigenetic changes, which are related to alterations in gene expression profiles. In addition, external factors such as viral infection can cooperate in the development of cancer. A subset of anogenital human papillomaviruses (HPVs), the high-risk HPVs (HR-HPVs), is associated with malignant tumors, including the majority of cervical cancers [1–3]. Cervical cancer is the second most common type of malignant lesion among women, with elevated mortality rates despite the increased screening efforts [4]. Prevention has recently been performed by prophylactic vaccines against the most abundant mucosal HR- and low-risk HPV types. However, the potential clinical benefit of prophylactic vaccines will not be apparent for several decades. In addition, due to their high cost, these vaccines have not been widely used in countries with the highest incidence of HR-HPVs-associated cancers. On the other hand, no HR-HPV specific antiviral treatments or therapeutic vaccines are currently available [5].

HR-HPV-associated cervical carcinogenesis is a multistep process, in which persistently infected cells develop first into precancerous lesions known as cervical intraepithelial neoplasia (CIN) [4]. A small percentage of these lesions (approximately 3%) progress to cervical carcinomas with more than half of them attributed to infection with HPV16 [3,6,7]. In HR-HPV associated cancers, E6 and E7 oncogenes target critical regulators of several cellular processes, resulting in alterations such as acquisition of unlimited proliferative potential, growth factor independence, evasion of

* Corresponding author. Address: Department of Genetics and Molecular Biology, Centro de Investigación y de Estudios Avanzados del IPN, Av. IPN 2508. Colonia San Pedro Zacatenco, CP 07360, Mexico DF, Mexico. Tel.: +52 55 57 47 3337; fax: +52 55 57 47 3931.
E-mail addresses: vidal@cinvestav.mx, wilox@cinvestav.mx (P. Gariglio).
[1] Present address: Cancer Cell Biology Laboratory, UACQB, Chilpancingo, Gro., Mexico.
[2] Present address: Department of Pharmaceutical Sciences, College of Pharmacy, OSU; Member, Environmental Health Science Center, OSU, Corvallis, OR 97331; Dept. of Dermatology, OHSU; Member, Knight Cancer Institute, OHSU, Portland, OR 97239, USA.

0304-3835/$ - see front matter © 2011 Elsevier Ireland Ltd. All rights reserved.
doi:10.1016/j.canlet.2011.11.031

apoptosis, lack of sensitivity to cytostatic signals, induction of invasive and metastatic properties, and sustained angiogenesis [8–14]. It has been demonstrated that the E6 and E7 oncoproteins act as potent mitotic mutators, thereby increasing the probability of acquiring cellular mutations that contribute to carcinogenic progression during each round of cell division [5]. E6 proteins from HR-HPVs target the tumor suppressor p53 for degradation, preventing cell growth inhibition in both undifferentiated and differentiated cells. HPV E7 protein binds to Rb family members and targets them for degradation. This results in the release and activation of E2F transcription factors that drive expression of S phase genes [2,5,15–19]. In addition, the *in vivo* properties of HR-HPV E6 and E7 oncoproteins have been evaluated through the generation and characterization of HPV transgenic mice strains [20–25].

Most cervical precancerous lesions containing HR-HPVs do not progress to invasive carcinomas, implicating that both genetic (cellular oncogenes or tumor suppressor gene mutations) and environmental cofactors (low dietary micronutrients such as vitamin A, chronic estrogen intake or other epigenetic regulators) could cooperate in those cases where cancer progression occurs [2,26–29].

Retinoid-induced differentiation is a cellular response that may be crucial for protection against cancer development. However, investigation of this process has so far been restricted to cultured cells [30–33] or to a few murine models that have been manipulated to conditionally delete RXRα in epidermal keratinocytes of adult mice [34,35]. In this conditional mouse model [RXRα (L-/L-)], temporally controlled epithelia-specific somatic mutagenesis of RXRα alleles results in severe skin abnormalities including alopecia, hyperproliferation, skin inflammatory reaction and aberrant terminal differentiation [36,37]. Moreover, in the same model, RXRα ablation was also demonstrated in cervical epithelial cells of adult mice, resulting in a simultaneous increase of cell proliferation and apoptosis levels accompanied by alteration in the expression of genes involved in both processes [38].

In order to investigate the role of HR-HPV oncogene expression in early cervical lesions *in vivo*, we produced a transgenic mouse expressing HPV16 E6 and E7 oncogenes from the promoter of the bovine keratin 6 gene [E6E7 (tg/0)]. These transgenic mice display a fur phenotype characterized by lower hair density and the ability to regenerate hair much faster than wild-type mice due to the inability to establish a resting telogen phase of hair follicle growth cycle [39], as well as tongue focal epithelial hyperplasia [40]. These mice also show a significantly higher number of putative epidermal stem cells as compared to wild-type mice, contributing to a faster wound re-epithelization [20]. Interestingly, these E6E7 (tg/0) mice showed low frequency of moderate and severe dysplasia (manuscript in preparation).

To study the possible cooperative effect between RXRα ablation and E6E7 expression to induce cervical malignant lesions, we produced a Triple Transgenic Mouse [TTM: RXRα-null conditional, expressing HPV16 E6E7 oncogenes; RXRα (Cvx L2/L2)/E6E7 (tg/0)]. Here we introduce a mouse model that, after RXRα ablation [RXRα (Cvx L-/L-)/E6E7 (tg/0)], develops spontaneously malignant cervical lesions allowing the study of the cooperative effect between HPV16E6E7 expression and the lack of RXRα in cervical cancer development.

2. Materials and methods

2.1. Generation of Tam-treated RXRα (L2/L2) [RXRα (Cvx L-/L-)], RXRα (Cvx L2/L2)/E6E7 (tg/0) mice (TTM) and Tam-treated RXRα (Cvx L-/L-)/E6E7 (tg/0) mice (Tam-TTM)

To carry out the conditional disruption of the RXRα gene in mouse cervical epithelia, the RXRα (L2/L2) conditional mouse line was constructed [35], in which the exon 4 is loxP-flanked (floxed) [36]. The generation of this floxed RXRα mouse line and genotyping using tail DNA have been described previously [35,41–43]. RXRα (L2/L2) conditional mice were Tam-treated as described previously [38] in order to generate RXRα (L-L-) mice. Three breeding pairs of RXRα (Cvx L2/L2) (C57BL/6xSJL strain) [44] and E6E7 (tg/0) (CD-1 strain) [39,40] mice were bred to produce multiple breeding pairs of RXRα (Cvx L2/L2)/E6E7 (tg/0) (TTM) mice. The genetic background of the line was mainly CD-1 strain (Fig. 1A). Mice were weaned at 21 days of age and fed with a fixed formula-autoclavable diet designed to support gestation, lactation, and growth of rodents (Teklad Global 18% Protein Rodent Diet; Harlan Teklad, Indianapolis, IN, USA). Animals were singly housed and kept under

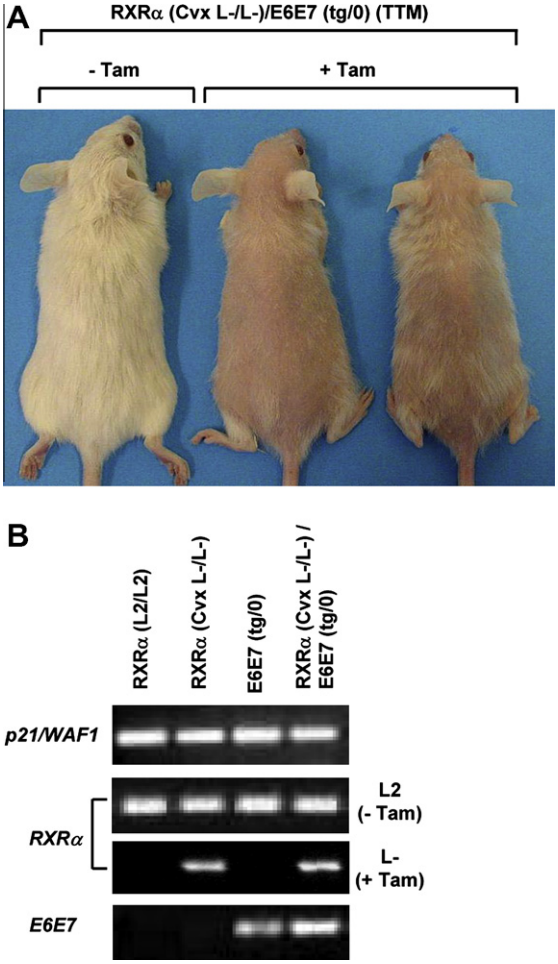

Fig. 1. (A) Representative images of untreated (-Tam) and Tam-treated (+Tam) RXRα (Cvx L-/L-)/E6E7 (tg/0) (Tam-TTM) mice. Tam-treated TTM showed smaller size and severe alopecia in comparison with untreated mice. (B) Evidence of floxed RXRα allele recombination (L-) after Tam treatment and presence of E6E7 transgene in mice strains included in this study. In order to confirm *in situ* analyses, we have performed traditional liquid phase PCR. Tail DNA was genotyped by PCR as described in Materials and Methods. The specific amplification products for RXRα or E6/E7 genes were separated by agarose gel electrophoresis and visualized by ethidium bromide staining. Cre-dependent recombination produces a null allele (L-) in Tam-treated RXRα (Cvx L-/L-) and Tam-treated RXRα (Cvx L-/L-)/E6E7 (tg/0) (Tam-TTM) mice. As expected, E6E7 transgene was detected only in E6E7 (tg0) and Tam-TTM mice. p21/WAF1: gene was used as amplification control to ensure the integrity of genomic DNA samples. (C) Tissue-specific RXRα gene ablation and efficient E6E7 oncogene expression. RXRα (PCR) panel: Detection of RXRα deletion by *in situ* PCR. Arrows indicate intense nuclear signal only in normal cervical epithelium (Open arrows) and stroma (Solid arrows) as indicated under Materials and Methods section. RXRα (RT-PCR) panel: Abrogation of RXRα mRNA production after RXRα gene ablation in cervix of mutant mice demonstrated by *in situ* RT-PCR. RXRα transcripts are present only in Tam-untreated epithelial cells (open arrows). As expected, no signal was detected for either RXRα gene (*in situ* PCR) or transcript (*in situ* RT-PCR) in epithelium of Tam-treated RXRα (Cvx L-/L-) and Tam-TTM mice. E6E7 (PCR) panel: *in situ* PCR for the detection of the E6E7 transgene. Open arrows indicate intense nuclear signal in E6E7 (tg/0) animals. E6E7 (RT-PCR) panel: E6E7 mRNA detection in cervix of transgenic mice and Tam-TTM demonstrated by *in situ* RT-PCR. E6E7 transgene and corresponding mRNA was detected only in cervix of E6E7 (tg/0) and Tam-TTM mice. BM: Basal Membrane. Magnification: 40X. Insets: 80 X. RXRα (L2/L2): Wild type mice; RXRα (Cvx L-/L-): Tam-treated RXRα conditional mice; E6E7 (tg/0): E6E7/HPV16 transgenic mice; RXRα (Cvx L-/L-)/E6E7 (tg/0): Tam-TTM. Scale bar, 50 μm.

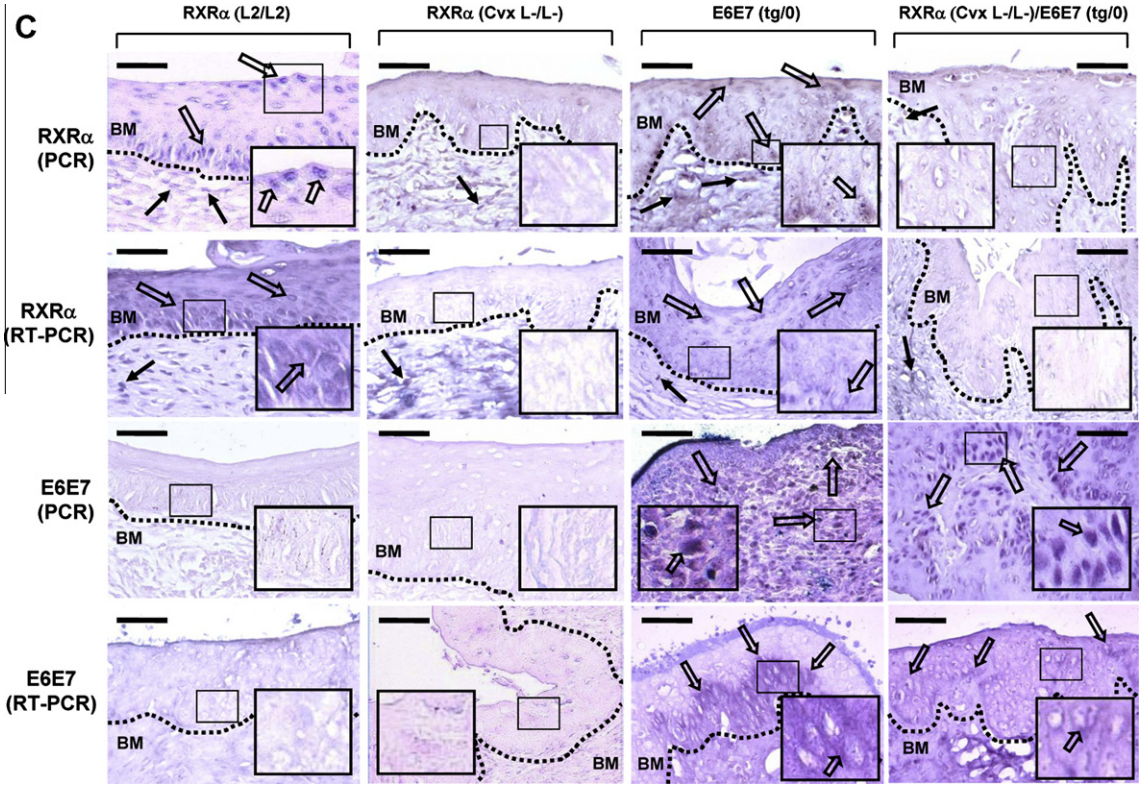

Fig. 1 (*continued*)

constant day-night (lights on 0630-1830) conditions. Four to six weeks-old mice were i.p.-injected with either vehicle (ethanol) or 0.1 mg Tamoxifen (Tam) per day for five consecutive days [35,38]. RXRα conditional animals without Tam treatment or Tam-treated Wild Type [RXRα (L2/L2); no Cre] animals were used as controls. Animals were sacrificed at least 21–23 weeks after Tam-treatment. All animal experiments were performed in compliance with the relevant laws and institutional guidelines and were approved by local animal ethics committee (UPEAL-CINVESTAV-IPN, Mexico; NOM-062-ZOO-1999).

2.2. Genotyping of the RXRα alleles

Genomic DNA was isolated as described [44]. To identify the recombined RXRα alleles, PCR was performed with primer ZO243 (5′-TCCTTCACCAAGCACATCTG-3′) (located in intron 3) and 3′-primer ZO244 (5′-TGCAGCCCTCACAACTGTAT-3′) (located in exon 4). These primers amplified Wild type (Wt) and L2 alleles (650 bp and 700 bp fragments, respectively [38]. UD196 primer (5′-CAACCTGGACTTGTCACTTAG-3′ is located in the intron 4 between Exon 4 and 5; this allele was used as *in situ* PCR amplification control [38] and for liquid phase PCR (Fig. 1B). To verify the excision efficiency of floxed RXRα alleles in cervical epithelium, PCR amplification was carried out in a buffer containing 10 mM Tris–HCl (pH 8.0), 50 mM KCl, 1.5 mM $MgCl_2$, 0.2 mM dNTPs, 0.25 μM of each primer, and 2 units of Taq polymerase (Invitrogen, USA) using 1 μg of genomic DNA as template. After 35 cycles (30 s at 94 °C, 30 s at 59 °C and 30 s at 72 °C) the products were analyzed on ethidium bromide-stained 2.5% agarose gels [38]. In all genotyping experiments it was included the amplification of a constitutive DNA sequence to ensure the integrity of genomic DNA samples (e.g. p21/WAF1 gene).

2.3. Genotyping of the E6E7 alleles

To identify the E6E7 alleles, both, liquid-phase PCR and *in situ* PCR were performed using E6E7 specific primers as previously described [40,45] (Fig. 1B).

2.4. Cervical tissue samples

Cervical tissue from mutant and control mice was dissected, fixed and paraffin-embedded as described elsewhere [46,47]. Briefly, mice were anesthetized with 2.5% Avertin and perfused through the aorta with 3.75% paraformaldehyde. The entire reproductive tract including parametrial, retroperitoneal soft tissue and lymph nodes were dissected, placed in an embedding cassette (Fisher, USA) with one sponge for compression, and postfixed in 3.75% paraformaldehyde overnight at 4 °C. In-cassette postfixation produced a linear reproductive tract facilitating subsequent sectioning of the entire organ in one plane [47]. The posterior vaginal wall was removed leaving an intact rim of vulvar tissue, and a 3–5 mm end piece of plastic pipette tip was inserted into the vagina to keep it open during subsequent processing steps. Tissues were washed in 1X PBS, and dehydrated through graded alcohols and xylene. After pipette tip removal, the reproductive tract was embedded with the cut vaginal wall surface oriented downward. The entire reproductive tract was serially sectioned (5 μm/section), and 10–15 sections were collected at 75 μm intervals for Hematoxylin staining, immunohistochemistry, *in situ* PCR and *in situ* RT-PCR. Five-micrometers-thick longitudinal sections were mounted on charged slides. All female mice were synchronized by exposure to the odor of a male, or to its urine (“Whitten effect”) [48]. Animals were sacrificed in estrous phase.

2.5. Histological analysis

For each specimen, 5-micron-thick histological sections were obtained to prepare distinct slides for light microscopy. The specimens stained with hematoxylin were evaluated by a pathologist. The histological criteria determined by the WHO were strictly followed in the analysis of the murine uterine cervix. The samples analyzed were obtained from: Wild type mice RXRα (L2/L2); Tam-treated RXRα conditional mice [RXRα (Cvx L-/L-)]; E6E7/HPV16 transgenic mice [E6E7 (tg/0)] and Tam-treated TTM [RXRα (Cvx L-/L-)/E6E7 (tg/0); Tam-TTM]. No defects or molecular alterations were observed in Wild type animals that received Tamoxifen or in Tam-untreated RXRα (L2/L2) animals.

2.6. Immunohistochemistry

Sections were deparaffinized and rehydrated as described previously [38,46]. Protein detection was performed using the Mouse/Rabbit PolyDetector HRP/DAB Detection System (Bio SB, USA). Briefly, tissues were rinsed in PBS and epitope retrieval was performed in a pressure cooker (121 °C, 20 lb of pressure) using the ImmunoRetriever Citrate Solution (Bio SB, USA) during 15 min. Slides were cooled at room temperature (30 min) and tissues were treated for 1 min with PolyDetector Peroxidase Block quenching buffer (Bio SB, USA). After three washes in PBS, sections were incubated 12–16 h at 4 °C with following primary antibodies: PCNA (cell proliferation marker) or HPV16 E6/HPV18 E6 (C1P5), mouse monoclonal antibody or $p16^{INK4A}$ (Santa Cruz Biotechnology, USA) or Cleaved Caspase 9 (apoptosis marker; Cell Signaling, USA) following manufacturer's recommended protocol. Following four washes in PBS, slides were incubated for 30 min with a secondary antibody (PolyDetector HRP label; Bio SB, USA). After three washes in PBS, sections were

incubated with appropriate substrate (PolyDetector DAB chromogen; Bio SB, USA), counterstained with hematoxylin and mounted in GVA-mount reagent (Zymed, USA). Negative controls included omission of primary antibody.

2.7. Apoptosis detection (TUNEL)

DNA fragmentation was assessed by TUNEL [49] according to the specifications of the manufacturer (Roche, USA). Briefly, paraffin tissue sections mounted on charged slides (5 μm thick) were deparaffinized with xylol, rehydrated and then deproteinated for 15 min (0.5 μg/mL Proteinase K in PBS), washed and dehydrated again. To avoid artificial DNA fragmentation, only nuclease-free solutions were used during the whole procedure. The labeling of 3′-OH ends of fragmented DNA was performed by incubation with fluorescein-dUTP using 12.5 U terminal deoxynucleotidyl transferase (TdT) for 1 h at 37 °C in a humidified chamber. As positive control, normal cervical tissue pre-treated with DNase I (4 U/tissue, 10 min at room temperature; Roche, USA) displayed nuclear positive reactivity in the majority of cells, demonstrating the incorporation of the fluorescent nucleotide at 3′-OH ends to the fragmented DNA. To estimate non-specific binding and autofluorescence, negative controls were included in all assays where tissue sections were incubated without the TdT enzyme. Slides were analyzed by fluorescence microscopy with a wide-band excitation barrier filter suitable for analyzing green (fluorescein labeled fragmented DNA) fluorescence. Three independent observers selected different optical fields in a random manner to determine the percentage of TUNEL positive staining in at least 500 cells for each sample. In addition, immunohistochemical detection of Cleaved Caspase 9 was performed as an apoptosis marker (see above in Section 2.6).

2.8. In situ PCR

In order to demonstrate: first, that RXRα gene, as well as the corresponding transcript, was ablated specifically in cervical epithelia of Tam-treated RXRα (Cvx L-/L-) mice and Tam-TTM and, second, that E6E7 transgene was present and the corresponding transcript was expressed in cervical epithelial cells of E6E7 (tg/0) mice and Tam-TTM, we decided to use both *in situ* PCR and *in situ* RT-PCR. These techniques combine the extreme sensitivity of PCR with the cell localizing ability similar to *in situ* hybridization and allow comparing epithelia with stroma. Direct *in situ* PCR was performed as previously described with some modifications [38,40,50]. Briefly, dried dewaxed sections on sylanecoated slides were incubated with protein lysis buffer (0.1 M Tris–HCl pH 8.0, 50 mM EDTA pH 8.0) containing 0.5 μg/ml Proteinase K for 30 min at room temperature. After thoroughly washing with DEPC-treated water, 50 μl of the PCR master mix solution containing digoxigenin-11-(2′-deoxy-uridine-5′)-triphosphate (DIG-11-dUTP; Roche, USA), were added. To reduce primer-dimer formation the PCR solution was heated to 70 °C for 10 min before Taq DNA polymerase (5 U per reaction) was added. Negative controls were made without primers or Taq. *In situ* PCR was performed using the system provided by Perkin Elmer (USA). The slides were preheated to 70 °C on the assembly tool included in the *in situ* Perkin Elmer equipment, 50 μl PCR master mix was added to each sample and the reaction was sealed using AmpliCover discs and clips (Perkin Elmer, USA). After assembly, slides were placed at 70 °C in the GeneAmp *In situ* PCR system 1000 (Perkin Elmer, USA) until running was started. PCR amplification was performed running 18 cycles as described previously [38,40]. Same primers were used for *in situ* amplification and Real Time analysis. After cycling was completed, the temperature was kept at 4 °C until disassembly. Clips were removed and AmpliCover discs were very carefully lifted from the slides without moving them sideways and slides were washed for 5 min in PBS followed by 5 min in 100% EtOH before they were air dried.

2.9. In situ RT-PCR

After Proteinase K digestion (see above), tissues were treated with 1 U/sample of DNase I, RNase-free (Roche, USA) during 48 h at room temperature. After thoroughly washing with DEPC-treated water, reverse transcription was performed using the SuperScript II reverse transcriptase (Invitrogen, USA), following the manufacturer's specifications. In brief, 70 μl DEPC-treated water containing 2.5 μg oligo$(dT)_{12\text{-}18}$, 10 mM dNTP mix (10 mM each dATP, dGTP, dCTP and dTTP at neutral pH), 5X first-strand buffer, 0.1 M DTT, recombinant ribonuclease inhibitor (40 U/μl) and reverse transcriptase (100 U/section) (Invitrogen, USA) were added to each section. Slides were incubated at 42 °C for 1 h in a sealed humidified chamber. After thorough washes, direct *in situ* PCR was performed using specific primers as described previously [38,40]. Negative controls included substituting one of the primers by H_2O in the PCR reaction or omission of the reverse transcription reaction.

2.10. Detection of in situ PCR products

An indirect immunolabeling method using a primary Anti-Digoxigenin antibody (Fab fragments; Roche, USA) conjugated to alkaline phosphatase was chosen to detect the PCR product. Briefly, blocking was carried out in 5% BSA (Sigma, USA) in PBS for 30 min. Slides were then drained and an Anti-DIG antibody diluted 1:200 in 100 mM Tris–HCl pH 7.4 and 150 mM NaCl, was applied (100 μl per sample) for 2 h at room temperature. As a negative control the primary antibody was omitted. Detection of alkaline phosphatase was carried out for 10–30 min using NBT/BCIP kit (Zymed, USA). After detection, slides were rinsed in distilled water for 5 min and air dried before mounting in Permount histological mounting medium (Fisher Scientific, USA).

2.11. Digital image capture, analysis and quantification

All photomicrographs were obtained using a DFC290 HD digital camera (Leica Microsystems, USA). The following method of quantification was used for immunohistochemical analyses. After acquisition of digital images, the experimental image files were opened in the PhotoImpact software (Ulead PhotoImpact SE version 3.02; Ulead Systems, USA). The images were digitally processed in order to obtain the better and homogeneous signal and then selected for analysis of relevant regions (cervical epithelium). The selected regions were then digitally analyzed using the Image-ProPlus Analysis Software (Ver 4.5.0.19, Media Cybernetics, Inc., USA). The amount of signal staining was quantified by calculating it as a pixel matrix data (the color contained within a pixel inside an image at specific location). Therefore, chromogen quantity was determined by calculating the norm of the matrix file for that image. This allows pixels of similar "color" immediately adjacent to the index pixel to be included for analysis. All pixels falling within the threshold parameters selected were quantified, recorded and used to generate a graphic. The file for the control image is generated similarly: the control slide is acquired and treated identically as the experimental slide except that negative controls were included (see above).

2.12. RNA isolation

Total RNA was isolated from cervical tissue obtained from mutant and control mice using TRIzol reagent according to the manufacturer's instructions (Invitrogen, USA). Tissues were obtained from female mice and stored at −80 °C. The quality of the total RNAs was examined by denaturing agarose gel electrophoresis and staining with ethidium bromide, and the 18S and 28S RNA bands were visualized by UV illumination. The concentrations of total RNA were quantified spectrophotometrically. The RNA preparations were used for quantitative Real-Time PCR (RTqPCR).

2.13. Preparation of cDNA for quantitative Real-Time PCR (RTqPCR)

Three micrograms of total RNA were reverse transcribed in a 20 μl reaction. The reaction mixture consisted of 5X first strand buffer [250 mM Tris–HCl (pH 8.3), 375 mM KCl, and 15 mM $MgCl_2$], 0.5 mM dNTPs, 5 mM dithiothreitol, 15 U RNase Inhibitor (Invitrogen, USA), 2.5 μg oligo$(dT)_{12\text{-}18,}$ and 100 U SuperScript II Reverse Transcriptase, following the manufacturer's specifications (Invitrogen, USA).

2.14. Relative mRNA quantification by RTqPCR

The relative quantification of the investigated mRNAs by RTqPCR was performed using a 7300 Real Time PCR System (Applied Biosystems, USA). Oligonucleotide primers were designed to be intron spanning and were purchased from Invitrogen, USA [38]. Sequences were obtained from the GenBank database. Optimal PCR reaction for all investigated genes was established using the SYBR Green PCR Master Mix (Applied Biosystems, USA) according to the manufacturer's instructions; annealing temperatures and $MgCl_2$ concentrations were optimized to create a one-peak melting curve. Additionally, the amplicons were checked by agarose gel electrophoresis for a single band of the expected size. PCRs were processed through 40 cycles of a 3-step PCR, including 10 s of denaturation at 95 °C, a 10-s primer dependent annealing phase (60 °C), and a 10 s template-dependent elongation at 72 °C. A 25 μl reaction consisted of 12.5 μl SYBR Green PCR Master Mix containing: Taq DNA polymerase, reaction buffer, dNTP mix and 1 mM $MgCl_2$ (final concentration), SYBR Green I dye, 0.5 μM of each primer, 1 μl template (1000 ng per reaction) and ultrapure water. The amplification of each template was performed in duplicate in one PCR run. To normalize for differences in the amount of cDNA added to the reactions, quantification of the housekeeping HPRT mRNA was performed as an endogenous control. The differential expression of the investigated genes was calculated as the ratio normalized to HPRT mRNA.

2.15. Statistical analysis

Data were compiled as mean ± S.D. For statistical analysis of differences between the groups, an unpaired Student's *t* test was performed. p values < 0.05 were considered to indicate significant differences between data sets.

3. Results

3.1. Efficient ablation of RXRα in the cervical epithelium of Tam-treated RXRα (Cvx L-/L)/E6E7 (tg/0) Triple Transgenic Mice (Tam-TTM)

Previously, spatially controlled targeted somatic mutagenesis systems have been developed in mice by cell-specific expression of the bacteriophage P1 Cre recombinase, which excises LoxP-flanked (floxed) DNA segments. Additionally, temporal control of Cre activity was obtained with conditional Cre recombinases resulting from fusions with mutated ligand binding domains of steroid receptors [44,51–53]. Thus, cell-specific expression of such fusion proteins between Cre and mutated ligand binding domains of the human estrogen receptor (Cre-ER^{T2}), whose activity is induced by the anti-estrogen Tamoxifen (Tam), has allowed efficient spatiotemporally controlled somatic mutagenesis of floxed target genes as RXRα in various cell types and tissues including cervical tissue [35,38]. We have obtained triple transgenic mice with CD1-like coat color, which developed severe alopecia after Tam-treatment (Fig. 1A). In order to detect both the RXRα recombined allele and the tissue-specific RXRα ablation in cervical epithelia we performed liquid phase PCR and *in situ* PCR analyses, respectively. Genotyping analyses showed that RXRα gene was efficiently deleted in RXRα (Cvx L-/L-) conditional mice and Tam-TTM (Fig. 1B). In addition, we demonstrated that RXRα^{L2} alleles were converted into RXRα^{L-} alleles in cervical epithelium but not in stroma of TTM (Fig. 1C), demonstrating the efficiency of Cre-ER^{T2} for mediating the selective somatic mutation of floxed RXRα in epithelia after Tam treatment. No L2 to L- allele conversion occurred in controls without Tam treatment or without loxP sites (e.g. Wild type and E6E7 (tg/0) mice; Fig. 1). As expected, we found that RXRα messenger RNA is absent in Tam-TTM in comparison with control mice (Fig. 1C, *in situ* RT-PCR panel).

3.2. The E6E7 transgene is expressed in cervix of E6E7 (tg/0) transgenic and Tam-TTM

Using liquid phase PCR, E6E7 transgene can be detected only in E6E7 (tg/0) transgenic mice and Tam-TTM (Fig. 1B). In order to demonstrate the presence of both the E6E7 transgene and its correspondent transcript in cervical tissue, we have used *in situ* PCR or *in situ* RT-PCR. As expected, intense amplification signal was detected only in epithelia of the cervix obtained from E6E7 (tg/0) transgenic mice and Tam-TTM (Fig. 1C). No evidence of E6E7 sequences was obtained in cervical tissue from wild type or Tam-treated RXRα Cvx L-/L- mice (Fig. 1C).

3.3. HPV-16 E6 oncoprotein detection and p16^{INK4A} expression in cervical tissue of E6E7 (tg/0) and TTM

As mentioned above, the E6E7 transgene and corresponding transcript was efficiently demonstrated in cervical tissue of E6E7 (tg/0) and Tam-TTM. In addition, HPV16-E6 protein expression was demonstrated in cervical tissue using immunohistochemical assays (Fig. 2). As indirect evidence of HPV16-E7 oncoprotein activ-

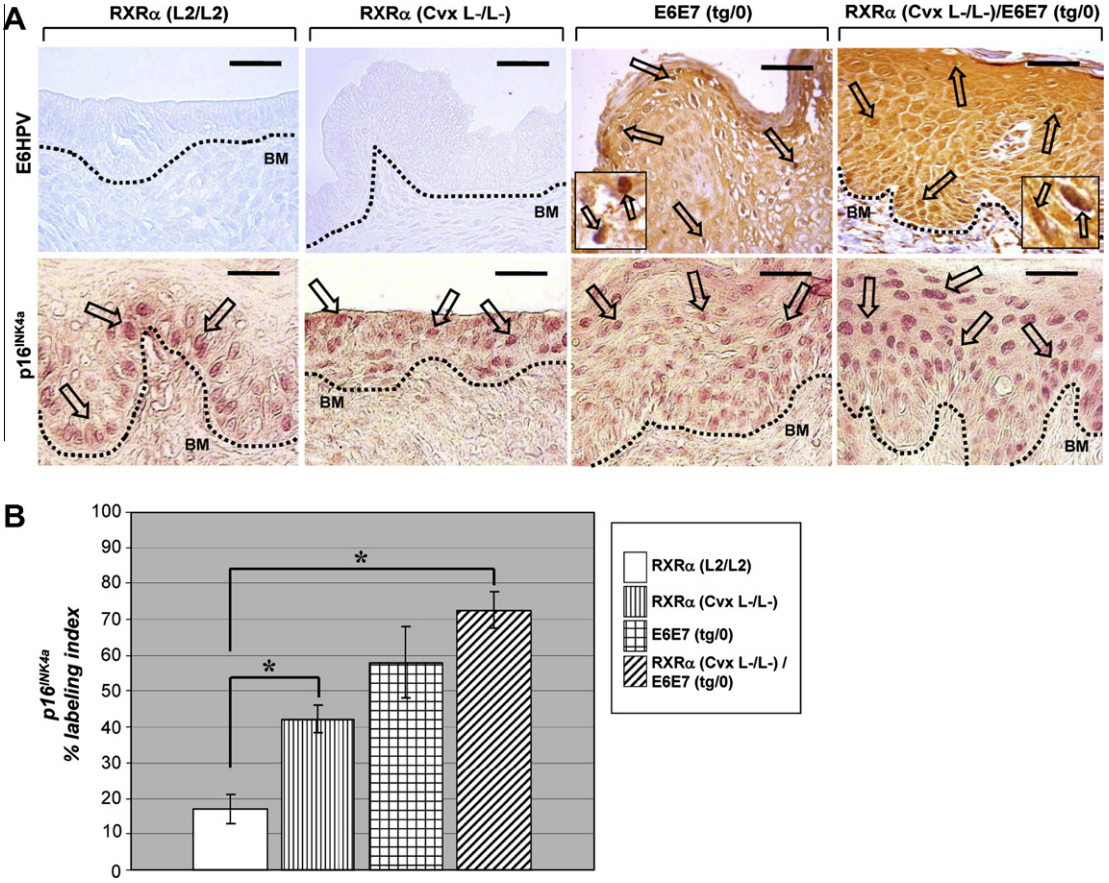

Fig. 2. E6 protein is expressed and p16^{INK4A} protein levels were increased in E6E7 murine cervix. (A) Immunohistochemical detection of E6 oncoprotein and p16^{INK4A} in cervical tissue. Open arrows indicate a nuclear HPV E6 or p16^{INK4A} strong positive signal. As expected, neither Tam-treated Wild type nor Tam-treated [RXRα (Cvx L-/L-)] conditional mice showed E6 expression, in comparison with Tam-treated TTM. (B) Relative expression (labeling index) of p16^{INK4A} in cervix of Wild type, Tam-treated mutant mice, E6E7 (tg/0) transgenic mice or Tam-treated TTM. Interestingly, p16^{INK4A} expression increased in Tam-treated RXRα conditional mice and was more abundant in TTM. BM: Basal Membrane. Magnification: 40X. Insets in E6HPV panel: 80X. RXRα (L2/L2): Wild type mice; RXRα (Cvx L-/L-): Tam-treated RXRα conditional mice; E6E7 (tg/0): E6E7/HPV16 transgenic mice; RXRα (Cvx L-/L-)/E6E7 (tg/0): Tam-treated TTM. *: Statistically significant ($P < 0.05$). Scale bar, 50 μm.

ity, we determined the levels of $p16^{INK4A}$, a tumor suppressor protein currently employed as a biomarker in human cervical cancer [54,55]. Cervical samples from E6E7 (tg/0) and Tam-treated TTM overexpressed $p16^{INK4A}$ as compared to cervical samples from Wild type control mice (Fig. 2B). Interestingly, RXRα ablation also induced $p16^{INK4A}$ protein overexpression in suprabasal layers (Fig. 2A and B).

3.4. Pathological changes in cervix of E6E7 (tg/0) transgenic mice and Tam-TTM

In order to determine histopathological changes associated with E6E7 expression, we performed analyses of cervical tissue obtained from middle age (27–29 weeks old) E6E7 (tg/0) transgenic mice. Interestingly, these mice showed a low frequency of moderate (2/44 mice; 0.9%) or severe (3/44 mice; 1.4%) dysplasia (Fig. 3A and Table 1). In addition, in order to determine whether RXRα ablation and the presence E6E7 played a role in the pathogenesis of cervical cancer, we performed similar histopathological evaluation of cervical tissue from Tam-TTM. Histological examination revealed that, after Tam treatment, cervix isolated from young TTM displayed moderate (11%) and severe (17%) dysplasia. Of interest, 61% (11/18) and 11% (2/18) of young Tam-TTM developed *in situ* carcinoma and invasive carcinoma, respectively (Fig. 3; Table 1).

3.5. Increase of cell proliferation levels and inhibition of apoptosis after RXRα ablation and E6E7 expression in the cervix of Tam-TTM

Previously, it was demonstrated that RXRα gene ablation induces both cell proliferation and apoptosis in cervical tissue [38]. Therefore, it was investigated the effect of both RXRα ablation and the presence of HPV E7/E7 on cell proliferation and apoptosis levels in cervix of Tam-TTM. Cell proliferation levels as determined by PCNA (Fig. 3B) and Ki-67 (not shown) nuclear cell counting, was higher for Tam-TTM than for untreated mice, RXRα (Cvx L-/L-) or E6E7 (tg/0) mice (PCNA and Ki67 levels were increased 5.6 and 5.9-fold in Tam-TTM, respectively as compared with Wild type controls; Fig. 3, B and D). As described previously, RXRα ablation increased the label index of apoptotic cells as determined by TUNEL and cleaved-Caspase 9 detection [38] (9.75 and 6.1-fold in RXRα (Cvx L-/L-) mice, respectively, as compared with Wild type controls; Fig. 4). Using the same strategy, Tam-TTM displayed the lowest apoptotic label index as compared to Wild type, RXRα Tam-treated conditional or E6E7 (tg/0) mice (Fig. 4).

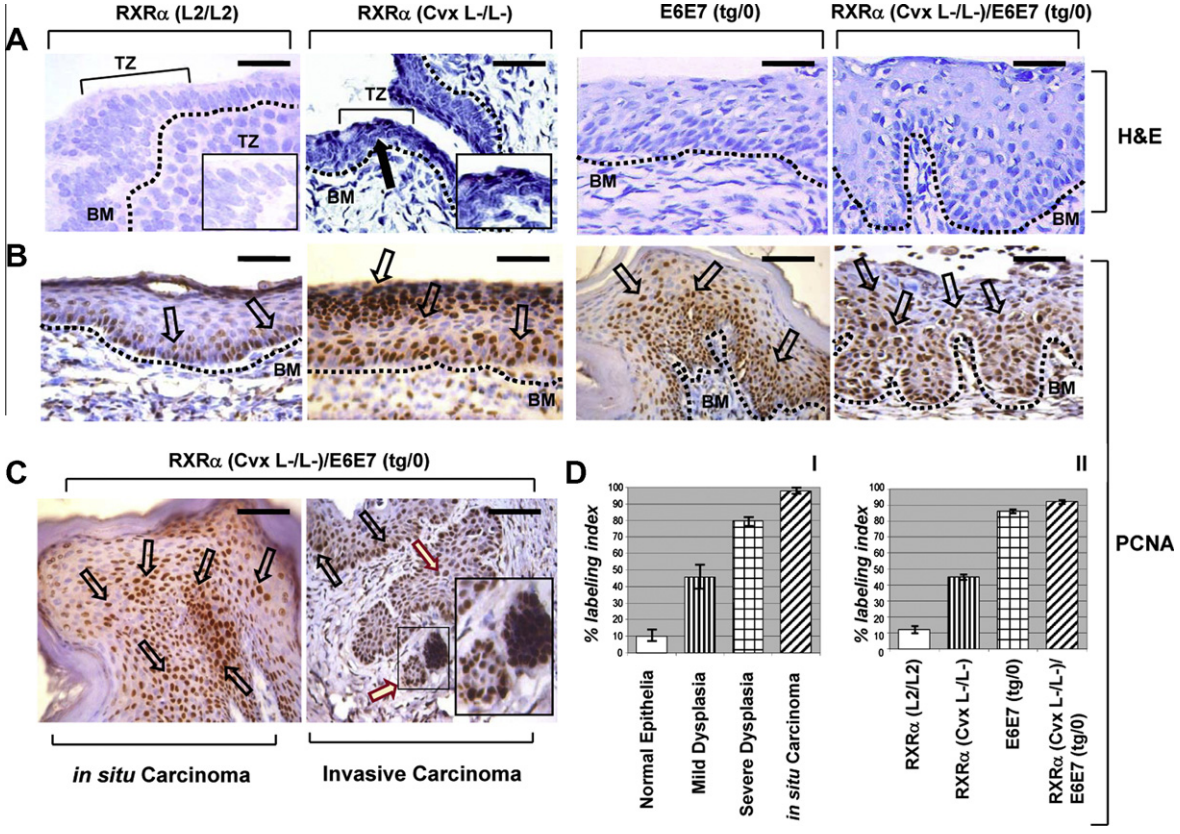

Fig. 3. Histological and proliferative alterations in cervical tissue after RXRα gene ablation and E6E7 viral oncoprotein expression. (A) Hematoxylin-Eosin (H&E) staining of cervical tissue from Wild Type, RXRα conditional, E6E7 (tg/0) transgenic and Tam-TTM. Wild Type mice [RXRα (L2/L2)] showed normal transformation zone (TZ) including cylindrical (columnar) single epithelium with transition to stratified (squamous) epithelium. Cervical tissue of Tam-treated RXRα mutant mice showed moderate epidermoid metaplasia (solid arrows). Interestingly, both E6E7 (tg/0) and Tam-treated TTM showed undifferentiated cells and hyperproliferation of the epithelia. (B) Immunohistochemical detection of PCNA as cell proliferation marker in cervix of Wild type, Tam-treated conditional and Tam-treated 7 month-old TTM. Cell proliferation levels were increased in RXRα (Cvx L-/L-), E6E7 (tg/0) transgenic and Tam-TTM as compared with controls. (C) Tam-treated TTM showed *in situ* carcinomas in 56% (10/18) of cervical samples and the development of frequent koilocyte-like cells (not shown). In addition, these Tam-treated TTM developed cervical invasive carcinoma after RXRα ablation in 11% (2/18) of the samples (red lined-yellow filled arrows). Open arrows: PCNA nuclear signal. BM: Basal Membrane. Magnification: 40X. Insets: magnification 80X. (D) Digital analysis of proliferation levels from murine cervical samples. After PCNA immunohistochemical detection, selected regions were digitally analyzed as described in Methods. (I) Relationship between labeling index (defined as percent of PCNA-positive cells) and histopathological diagnosis. It can be observed that there exists a correlation between increases in cell proliferation (that is, labeling index) and severity of the cervical lesions. Interestingly, in (II) we observed that the increase in cell proliferation depends on the genotype of the mice strain. RXRα (L2/L2): Wild type mice; RXRα (Cvx L-/L-): Tam-treated RXRα conditional mice; E6E7 (tg/0): E6E7/HPV16 transgenic mice; RXRα (Cvx L-/L-)/E6E7 (tg/0): Tam-treated TTM. Scale bar, 50 μm.

Table 1
Histological analysis of cervical tissues[a].

Genotype	Histopathological diagnosis	%
RXRα (L2/L2) ($n = 12$)	Normal epithelia	84
	Keratinized epithelia	8
	Mild dysplasia	8
RXRα (Cvx L-/L-)[b] ($n = 15$)	Epidermoid metaplasia	47
	Moderate dysplasia	40
	Cervicitis	13
E6E7 (tg/0)[c] ($n = 44$)	Moderate dysplasia	0.9
	Severe dysplasia	1.4
TTM RXRα (Cvx L-/L-)/E6E7 (tg/0) ($n = 18$)	Invasive cancer	11
	in situ carcinoma	61
	Severe dysplasia	17
	Moderate dysplasia	11

[a] All mice were treated with 0.1 mg Tam per day for five consecutive days.
[b] RXRα (Cvx L-/L-) mice showed cervical atrophy in 60% (9/15) of the samples.
[c] For this study it was included only the group of E6E7 (tg/0) transgenic mice that showed histopathological cervical alterations.

3.6. The levels of c-myc, Bax, Bcl-2 and p21WAF1 mRNA in E6E7 (tg/0) transgenic and Tam-TTM

According to the findings related to cell proliferation and apoptosis, we investigated the expression levels of selected genes by quantitative Real Time PCR (RTqPCR; Fig. 5). We found that c-myc, p21/WAF1 and Bcl-2 mRNA levels were increased mainly in Tam-TTM as compared to Tam-treated Wild type, RXRα (Cvx L-/L-) or E6E7 (tg/0) mice. In addition, in Tam-treated RXRα conditional mice, Bcl-2 and p21WAF1 expression were diminished, suggesting that RXRα absence can mediate both a proliferative and apoptotic effect in cervical tissue. Thus, despite the increased levels of p21/WAF1 expression, the presence of E6 and E7 oncoproteins in E6E7 (tg/0) transgenic mice and Tam-TTM not only increased the proliferative effect in cervical tissue, but also diminished the apoptotic levels. Strikingly, E6E7 oncogene expression was sufficient to abolish the effects of the RXRα ablation, drastically bringing down the apoptotic levels in Tam-TTM.

4. Discussion

4.1. RXRα gene ablation increases the apoptotic levels in the cervix of RXRα (Cvx L-/L-) mice

Histological analyses, after Tam induced ablation of RXRα gene in cervical epithelia [thereafter RXRα (Cvx L-/L-) mice] revealed that the cervical epithelium from RXRα mutant mice was thinner than control epithelium (atrophy). Although the ablation of RXRα gene increases cervical cell proliferation (see later), we have observed an increase in the activation of Caspase 9 in cervical epithelium of RXRα mutant mice compared with control mice (Fig. 4). It is known that Caspase 9 activation is a key event during the induction of apoptosis through the intrinsic pathway [17,56]. These results suggest that high apoptosis levels observed under this condition are probably preventing tissue hyperproliferation due to a decrease in the number of suprabasal layers and leading to an atrophy-like phenotype (Figs. 3 and 4).

4.2. HPV E6 and E7 expression decrease the apoptotic levels in cervix of E6E7 transgenic mice and Tam-TTM

Consistent with previous observations [18,57,58], in this work we found that E6 and E7 expression inhibit apoptosis levels in the cervix of both E6E7 transgenic mice and Tam-TTM, suggesting that death programming is abrogated in cervical tissue of Tam-TTM mice (Fig. 4). Thus, apoptosis inhibition might cooperate with the increase in cervical cell proliferation induced by RXRα ablation in Tam-TTM. It is well known that Bcl-2 promotes cell survival, whereas Bax promotes cell death [59] and that the ratio of Bcl-2/Bax determines survival or death following an apoptotic stimulus [60]. Thus, decrease of Bcl-2/Bax ratio observed after RXRα ablation should dramatically increase cell death in RXRα mutant mice. In contrast, the Bcl-2/Bax ratio was increased in both E6E7 (tg/0) transgenic and Tam-TTM in comparison with Wild type animals. It is noteworthy that in the cervix of E6E7 (tg/0) mice and Tam-TTM, only a twofold increase in Bcl-2/Bax ratio (in comparison with RXRα mutant mice) was observed that could hardly explain the dramatic decrease in cell death. This situation probably contributes to the reduction in apoptotic index observed in cervical tissues from both E6E7 (tg/0) transgenic mice and Tam-TTM (Fig. 5 and 6). It is important to mention that no definitive conclusion can be attained since levels of Bcl-2 and Bax proteins may not correlate with the mRNA levels due to the effects of E6 or E7 on the respective proteins [17,61].

E6 inactivation of p53 protein might result in overexpression of Bcl-2 and down regulation of Bax and Bak [17,62–67,68–74], contributing to continuous cell accumulation in cervix of E6E7 (tg/0) mice and Tam-TTM. In addition, HPV16 E6 blocks TNF-mediated cytolysis in mouse fibroblasts [75]. Thus, continuous presence of E6 is important for the viability of HPV-positive cancer cells, defining E6 as a promising target for therapeutic intervention. Moreover, ectopically expressed E6 has been associated with the inhibition of a wide range of different proapoptotic regulators that belong to the extrinsic death-receptor pathway (e.g. CD95 or FADD) and to the intrinsic mitochondrial pathway (e.g. Bax or Bak). It is also possible that E6 activates antiapoptotic molecules common to both pathways, such as the c-IAP2 and Bcl-2 proteins [17,74,76,77] (Fig. 6).

4.3. Cell proliferation levels are increased in cervical epithelium of RXRα (Cvx L-/L-) and Tam-TTM mice

Analyses of cell proliferation levels (PCNA expression) revealed presence of abundant proliferative cells in all layers of the stratified cervical epithelia from Tam-TTM, whereas the signal was found essentially in the basal layer of Wild type mice. In contrast, a modest increase in proliferative index was observed in cervical tissue from RXRα (Cvx L-/L-) mice while only few E6E7 (tg/0) mice showed an increase in cell proliferation levels (Fig. 3). This observation is consistent with higher levels of PCNA expression reported in E7-expressing keratinocytes compared to wild-type keratinocytes [58] and also in HR-HPV positive human cervical samples [78]. Our results suggest that in Tam-TTM, RXRα ablation and E6/E7 expression cooperatively contribute to increased proliferation activity and possibly to altered terminal differentiation of the cervical epithelium (Fig. 3 and 6).

4.4. $p16^{INK4A}$ cervical cancer biomarker is increased in RXRα (Cvx L-/L-) mice and Tam-TTM

Overexpression of tumor suppressor $p16^{INK4A}$ is associated with high-grade precancerous lesions and cervical carcinomas, and it has been demonstrated that immunohistochemical evaluation of this protein might be useful biomarker for identifying HR-HPV infected high-grade lesions [79]. The $p16^{INK4A}$ protein blocks cdk4 and cdk6-mediated pRb phosphorylation, resulting in inhibition of both E2F dependent transcription and cell cycle progression at the G1 to S checkpoint [79,80]. During cervical carcinogenesis there is an activation of both E2F and cell cycle progression since E7 inactivates pRb [80]. In this case it seems that the release of E2F activates the $p16^{INK4A}$ promoter. Interestingly, ablation of

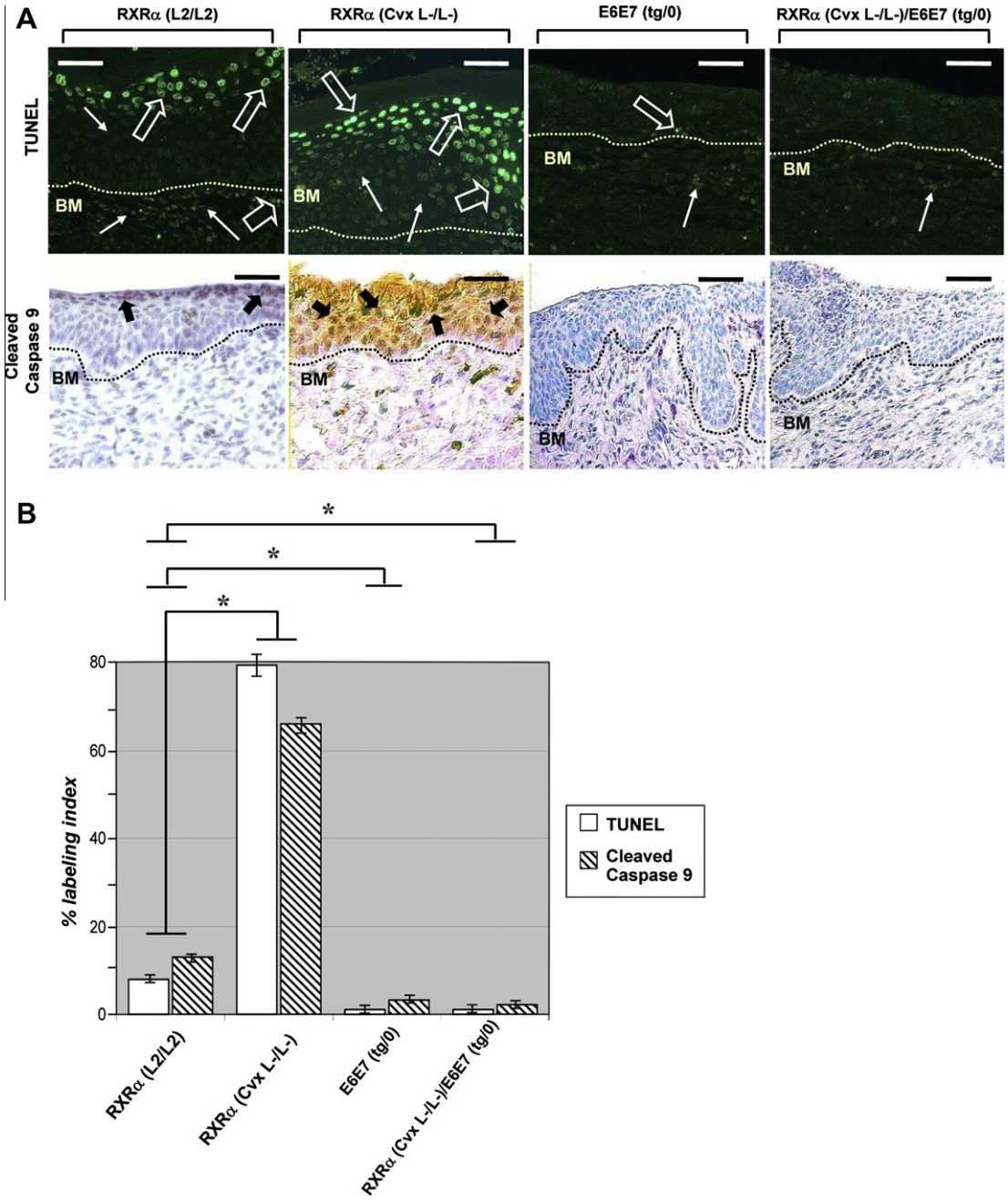

Fig. 4. Apoptotic levels in cervix of RXRα mutant mice were strongly reduced by E6E7 oncoprotein expression. (A) Apoptotic levels were measured in cervix of Wild type, RXRα (Cvx L-/L-), E6E7 (tg/0) transgenic mice and Tam-TTM, using TUNEL analysis and immunohistochemical detection of Cleaved Caspase 9. As images show, low apoptosis levels were detected in E6E7 (tg/0) and Tam-TTM as compared with either Wild type or RXRα mutant mice. TUNEL Panel: Solid arrows: non-apoptotic cells; Open arrows: apoptotic cells. Cleaved Caspase 9 Panel: Solid arrows: apoptotic cells. BM: Basal Membrane. Magnification 40X. (B) Digital analysis of apoptotic levels in cervical samples from Fig. 4A. After apoptosis determination assays, selected representative regions were digitally analyzed and reported as labeling index (defined as percent of TUNEL or Cleaved Caspase 9-positive cells). Diminished apoptosis levels in cervix resected from E6E7 (tg/0) and Tam-TTM were clearly observed; Tam-TTM showed the lowest percentage of TUNEL and Cleaved Caspase 9 positive cells. RXRα (L2/L2): Wild type mice; RXRα (Cvx L-/L-): Tam-treated RXRα conditional mice; E6E7 (tg/0): E6E7/HPV16 transgenic mice; RXRα (Cvx L-/L-)/E6E7 (tg/0): Tam-treated TTM. ∗: Statistically significant ($P < 0.05$). Scale bar, 50 μm.

RXRα gene in cervix of RXRα (Cvx L-/L-) induced $p16^{INK4A}$ protein overexpression (Fig. 2), This suggests that the lack of this retinoid receptor could increase the release of E2F transcription factor activating the $p16^{INK4A}$ promoter [81] or induce epigenetic reprogramming of the $p16^{INK4A}$ promoter [81,82]. It is well known that in most cervical carcinomas, overexpression of $p16^{INK4A}$ indicates persistent infection with HR-HPV. Of relevance in this context is the observation that $p16^{INK4A}$ induction was elevated in cervical lesions arising in Tam-TTM (Fig. 2), which suggests that TTM strain might resemble persistent HR-HPV infection in humans. It has been described that E7 associates and inactivates E2F6 and Bmi1 (member of the polycomb group transcription repressors), both proteins being transcriptional repressors of $p16^{INK4A}$ [18,81–84]; repressive trimethyl marks on lysine 27 of histone 3 (H3), which are necessary for binding of polycomb repressive complexes, are decreased in HPV16 E7-expressing cells and HPV16-positive cervical lesions. This depletion of H3K27 methylation is caused by transcriptional induction of the KDM6B H3 lysine 27-specific demethylase. In addition, it was shown that E7-mediated $p16^{INK4A}$ induction is independent of pRb inactivation and is mediated by

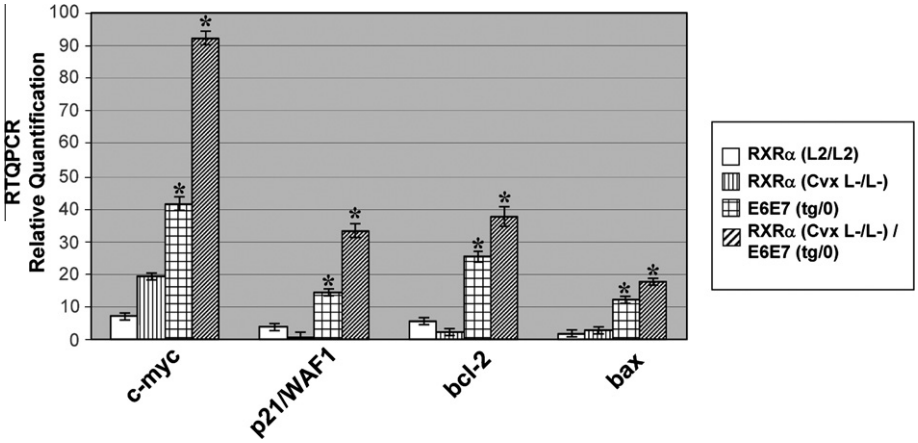

Fig. 5. Relative expression (RTqPCR) of genes involved in cell proliferation and apoptosis, in cervix of mice models. The level of selected transcripts involved in cell proliferation and/or apoptosis (c-myc, p21/WAF1, Bcl-2 and Bax) was assessed by RTqPCR using specific primers. RXRα (L2/L2): Wild type mice; RXRα (Cvx L-/L-): Tam-treated RXRα conditional mice; E6E7 (tg/0): E6E7/HPV16 transgenic mice; RXRα (Cvx L-/L-)/E6E7 (tg/0): Tam-treated TTM. *: Statistically significant ($P < 0.05$).

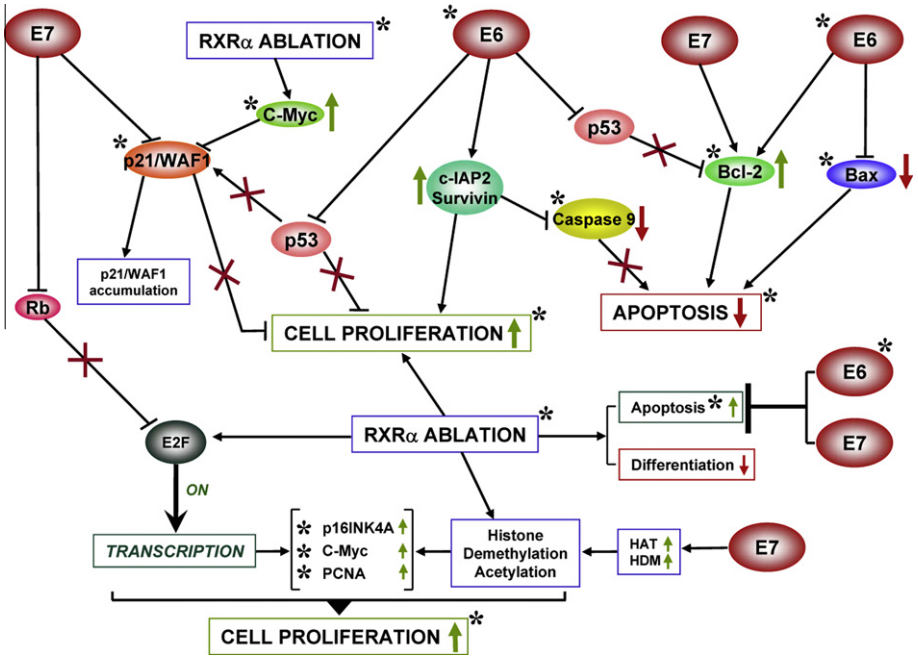

Fig. 6. Model for the concerted action of HPV E6/E7 oncogene expression and RXRα ablation in Triple Transgenic Mice. RXRα deletion induces cervical cell proliferation and blocks differentiation mechanisms cooperating with cellular transformation. E6 and E7 oncoproteins can cooperatively induce an increase of cell survival and cell proliferation levels. In sum, it is proposed that the development of *in situ* carcinoma and invasive cervical cancer in middle age Tam-TTM is induced by alteration of several cell control mechanisms. For details see Discussion. Up arrows: indicate overexpression or activated pathway. Down arrows: indicate underexpression. *: Molecules or cellular processes analyzed in this work. HAT: Histone acetyltransferase. HDM: Histone demethylase.

KDM6B [82]. This raises the interesting possibility that RXRα ablation causes the transcriptional induction of the KDMB6 demethylase, cooperating with E7-induced overexpression of $p16^{INK4A}$.

4.5. Gene expression levels of a set of genes associated with cervical carcinogenesis

In the present study, we analyzed the expression of a set of genes that are differentially expressed during cell proliferation and/or apoptosis and have a known association with cervical carcinogenesis [38]. For example, increased C-Myc expression was observed in RXRα (Cvx L-/L-) conditional, E6E7 (tg/0) transgenic and Tam-TTM when compared with expression in the wild type mice (Fig. 5). It has been reported that retinoids convert E2F into a transcriptional suppressor inhibiting the transcription of several target genes including C-Myc [85]. Increased levels of C-Myc mRNA after RXRα ablation in cervical epithelia could be partially due to the lack of E2F repressive activity and can be associated with uncontrolled cellular proliferation in Tam-TTM (Fig. 6) [86–89]. p21/WAF1, which has been shown to induce G1 arrest by inhibition of cyclin-dependent kinases, has been identified as one of the wild-type p53-activated genes [90,91]. The repression of p21/WAF1 mRNA expression observed after RXRα ablation (Fig. 5), may partially explain the increase in cervical cell proliferation in RXRα (Cvx L-/L-) mice, suggesting that RXRα signaling is crucial for the negative regulation of the cell cycle and for cervical homeostasis. The E7 oncoprotein can override p21/WAF1 inhibition of both CDK activity and proliferating cell nuclear antigen (PCNA)-dependent DNA synthesis [18,57]. The relationship between E7 and p21WAF1 is paradoxical because E7 causes an increased level

of p21/WAF1 protein in human and mouse cells/tissues [18,58,92] and at the same time E7 can inactivate p21/WAF1 [18,57,58]. Accordingly, p21/WAF1 was overexpressed in Tam-TTM cervix as compared to normal cervical tissue probably due to E7 oncoprotein expression. These data suggest that, in the Tam-TTM model, RXRα ablation and E6 together with E7 expression cooperatively increased the frequency of pre-malignant or malignant cervical lesions inactivating the tumor suppressor function of p21/WAF1 and inducing cervical carcinogenesis.

The main finding of this work was the detection of *in situ* carcinoma (61%) and invasive carcinoma (11%) in the cervix of middle age Tam-treated TTM, suggesting that lack of RXRα retinoid receptor coupled with expression of HPV16 E6 and E7 oncoproteins may contribute to carcinogenesis. Our findings suggest that induction of cervical cancer in Tam-treated TTM could prove a valuable model for the diagnosis and prognosis of cancer. The TTM model can be further utilized to identify cofactors involved in cervical carcinogenesis. The use of a conditionally expressed retinoid receptor in mice that express HR-HPV16 E6E7 oncoproteins, may improve future studies by allowing the identification of early tumoral biomarkers during the development of cervical cancer.

Acknowledgements

We are grateful to Dr. Pierre Chambon and Dr. Daniel Metzger (IGBMC, CNRS, INSERM, Université Louis Pasteur, Illkirch-Cedex, Strasbourg, France) for the kind gift of their invaluable RXRα conditional mouse model and for helpful discussions. We would like to thank Dr. Diana Escalante-Alcalde (IBT-UNAM), Biol. Elizabeth Alvarez, Biol. Enrique García and Mr. Lauro Macías (CINVESTAV-IPN, Mexico) for technical support. This work was supported by CONACyT (Mexico) and ICGEB, CRP Programme, Trieste, Italy. PG was supported by a UICC Translational Cancer Research Fellowship, funded by Novartis (Switzerland). ECS was supported by the scholarship "Ligue Contre le Cancer comité de Bas-Rhin".

References

[1] H. zur Hausen, Papillomavirus infections: a major cause of human cancer, Biochim. Biophys. Acta 1288 (1996) F55–F78.
[2] H. zur Hausen, The search for infectious causes of human cancers: where and why (Nobel lecture), Angew Chem. Int. Ed. Engl. 48 (2009) 5798–5808.
[3] J.M. Walboomers, M.V. Jacobs, M.M. Manos, F.X. Bosh, J.A. Kummer, K.V. Shah, P.J. Snijders, J. Peto, C.J. Meijer, N. Muñoz, Human papillomavirus is a necessary cause of invasive cervical cancer worldwide, J. Pathol. 189 (1999) 12–19.
[4] R. Sankaranarayanan, J. Ferlay, Worldwide burden of gynaecological cancer: the size of the problem, Best. Pract. Res. Clin. Obstet. Gynaecol. 20 (2006) 207–225.
[5] M.E. McLaughlin-Drubin, K. Münger, Oncogenic activities of human papillomaviruses, Virus Res. 143 (2009) 195–208.
[6] A.B. Moscicki, Impact of HPV infection in adolescent populations, J. Adolesc. Health 37 (2005) S3–S9.
[7] F.X. Bosch, A. Lorincz, N. Munoz, C.J. Meijer, K.V. Shah, The causal relation between human papillomavirus and cervical cancer, J. Clin. Pathol. 55 (2002) 244–265.
[8] D. Hanahan, R.A. Weinberg, The hallmarks of cancer, Cell 100 (2000) 57–70.
[9] C.D. Woodworth, J. Doniger, J.A. DiPaolo, Immortalization of human foreskin keratinocytes by various human papillomavirus DNAs corresponds to their association with cervical carcinoma, J. Virol. 63 (1989) 159–164.
[10] A.J. Van den Brule, F.V. Cromme, P.J. Snijders, L. Smit, C.B. Oudejans, J.P. Baak, C.J. Meijer, J.M. Walboomers, Nonradioactive RNA in situ hybridization detection of human papillomavirus 16-E7 transcripts in squamous cell carcinomas of the uterine cervix using confocal laser scan microscopy, Am. J. Pathol. 139 (1991) 1037–1045.
[11] M.A. Bedell, K.H. Jones, S.R. Grossman, L.A. Laimins, Identification of human papillomavirus type 18 transforming genes in immortalized and primary cells, J. Virol. 63 (1989) 1247–1255.
[12] W.C. Phelps, C.L. Yee, K. Münger, P.M. Howley, The human papillomavirus type 16 E7 gene encodes transactivation and transformation functions similar to those of adenovirus E1A, Cell 53 (1988) 539–547.
[13] A. Storey, D. Pim, A. Murray, K. Osborn, L. Banks, L. Crawford, Comparison of the in vitro transforming activities of human papillomavirus types, EMBO J. 7 (1988) 1815–1820.
[14] A. Storey, L. Banks, Human papillomavirus type 16 E6 gene cooperates with EJ-ras to immortalize primary mouse cells, Oncogene 8 (1993) 919–924.
[15] C.A. Moody, L.A. Laimins, Human papillomavirus oncoproteins: pathways to transformation, Nat. Rev. Cancer 10 (2010) 550–560.
[16] A.F. Nicol, G.J. Nuovo, J. Dillner, A summary of the 25th International Papillomavirus Conference 2009: vaccines, screening, epidemiology and therapeutics, J. Clin. Virol. 47 (2010) 208–215.
[17] M. Lagunas-Martínez, V. Madrid-Marina, P. Gariglio, Modulation of apoptosis by early human papillomavirus proteins in cervical cancer, Biochim. Biophys. Acta 1805 (2010) 6–16.
[18] M.K. Shin, S. Balsitis, T. Brake, P.F. Lambert, Human papillomavirus E7 oncoprotein overrides the tumor suppressor activity of p21Cip1 in cervical carcinogenesis, Cancer Res. 69 (2009) 5656–5663.
[19] S.S. Tungteakkhun, P.J. Duerksen-Hughes, Cellular binding partners of the human papillomavirus E6 protein, Arch. Virol. 153 (2008) 397–408.
[20] C. Valencia, J. Bonilla-Delgado, K. Oktaba, R. Ocadiz-Delgado, P. Gariglio, L. Covarrubias, Human papillomavirus E6/E7 oncogenes promote mouse ear regeneration by increasing the rate of wound re-epithelization and epidermal growth, J. Invest. Dermatol. 128 (2008) 2894–2903.
[21] R.L. Eckert, J.F. Crish, S. Balasubramanian, E.A. Rorke, Transgenic animal models of human papillomavirus-dependent disease, Int. J. Oncol. 16 (2000) 853–870.
[22] J.K. Wolf, E.L. Franco, J.M. Arbeit, K.R. Shroyer, T.C. Wu, C.D. Runowicz, G. Tortolero-Luna, R. Herrero, C.P. Crum, Innovations in understanding the biology of cervical cancer, Cancer 98 (2003) 2064–2069.
[23] S.H. Chung, P.F. Lambert, Prevention and treatment of cervical cancer in mice using estrogen receptor antagonists, Proc. Natl. Acad. Sci. USA 106 (2009) 19467–19472.
[24] S.F. Jabbar, L. Abrams, A. Glick, P.F. Lambert, Persistence of high-grade cervical dysplasia and cervical cancer requires the continuous expression of the human papillomavirus type 16 E7 oncogene, Cancer Res. 69 (2009) 4407–4414.
[25] A. Shai, H.C. Pitot, P.F. Lambert, E6-associated protein is required for human papillomavirus type 16 E6 to cause cervical cancer in mice, Cancer Res. 70 (2010) 5064–5073.
[26] X. Castellsagué, N. Muñoz, Cofactors in human papillomavirus carcinogenesis–role of parity, oral contraceptives, and tobacco smoking, J. Natl. Cancer Inst. Monogr. 31 (2003) 20–28. Chapter 3.
[27] N. Muñoz, X. Castellsagué, A.B. de González, L. Gissmann, Chapter 1: HPV in the etiology of human cancer, Vaccine 24 (2006) S3/1-10. Chapter 1.
[28] W.K. Huh, Human papillomavirus infection: a concise review of natural history, Obstet. Gynecol. 114 (2009) 139–143.
[29] P. Gariglio, J. Gutiérrez, E. Cortés, J. Vázquez, The role of retinoid deficiency and estrogens as cofactors in cervical cancer, Arch. Med. Res. 40 (2009) 449–465.
[30] J. Abu, M. Batuwangala, K. Herbert, P. Symonds, Retinoic acid and retinoid receptors: potential chemopreventive and therapeutic role in cervical cancer, Lancet Oncol. 6 (2005) 712–720.
[31] P. Germain, P. Chambon, G. Eichele, R.M. Evans, M.A. Lazar, M. Leid, A.R. De Lera, R. Lotan, D.J. Mangelsdorf, H. Gronemeyer, International union of pharmacology. LX. Retinoic acid receptors, Pharmacol. Rev. 58 (2006) 712–725.
[32] D.R. Soprano, B.W. Teets, K.J. Soprano, Role of retinoic acid in the differentiation of embryonal carcinoma and embryonic stem cells, Vitam. Horm. 75 (2007) 69–95.
[33] N.P. Mongan, L.J. Gudas, Diverse actions of retinoid receptors in cancer prevention and treatment, Differentiation 75 (2007) 853–870.
[34] A.K. Indra, X. Warot, J. Brocard, J.M. Bornert, J.H. Xiao, P. Chambon, D. Metzger, Temporally-controlled site-specific mutagenesis in the basal layer of the epidermis: comparison of the recombinase activity of the tamoxifen-inducible Cre-ER(T) and Cre-ER(T2) recombinases, Nucleic Acids Res. 27 (1999) 4324–4327.
[35] D. Metzger, A.K. Indra, M. Li, B. Chapellier, C. Calleja, N.B. Ghyselinck, P. Chambon, Targeted conditional somatic mutagenesis in the mouse: temporally-controlled knock out of retinoid receptors in epidermal keratinocytes, Methods Enzymol. 364 (2003) 379–408.
[36] M. Li, A.K. Indra, X. Warot, J. Brocard, N. Messaddeq, S. Kato, D. Metzger, P. Chambon, Skin abnormalities generated by temporally controlled RXRalpha mutations in mouse epidermis, Nature 407 (2000) 633–636.
[37] A.K. Indra, E. Castaneda, M.C. Antal, M. Jiang, N. Messaddeq, X. Meng, C.V. Loehr, P. Gariglio, S. Kato, W. Wahli, B. Desvergne, D. Metzger, P. Chambon, Malignant transformation of DMBA/TPA-induced papillomas and nevi in the skin of mice selectively lacking retinoid-X-receptor alpha in epidermal keratinocytes, J. Invest. Dermatol. 127 (2007) 1250–1260.
[38] R. Ocadiz-Delgado, E. Castaneda-Saucedo, A.K. Indra, R. Hernandez-Pando, P. Gariglio, Impaired cervical homeostasis upon selective ablation of RXRalpha in epithelial cells, Genesis 46 (2008) 19–28.
[39] D. Escalante-Alcalde, F. Recillas-Targa, C. Valencia, J. Santa-Olalla, P. Chávez, A. Marroquín, X. Gutiérrez, P. Gariglio, L. Covarrubias, Expression of E6 and E7 papillomavirus oncogenes in the outer root sheath of hair follicles extends the growth phase and bypasses resting at telogen, Cell Growth Differ. 11 (2000) 527–539.
[40] R. Ocadiz-Delgado, A. Marroquin-Chavira, R. Hernandez-Mote, C. Valencia, M.E. Manjarrez-Zavala, L. Covarrubias, P. Gariglio, Induction of focal epithelial hyperplasia in tongue of young bk6-E6/E7 HPV16 transgenic mice, Transgenic Res. 18 (2009) 513–527.
[41] M. Schuler, A. Dierich, P. Chambon, D. Metzger, Efficient temporally controlled targeted somatic mutagenesis in hepatocytes of the mouse, Genesis 39 (2004) 167–172.

[42] M. Li, H. Chiba, X. Warot, N. Messaddeq, C. Gerard, P. Chambon, D. Metzger, RXR-alpha ablation in skin keratinocytes results in alopecia and epidermal alterations, Development 128 (2001) 675–688.
[43] J. Brocard, X. Warot, O. Wendling, N. Messaddeq, J.L. Vonesch, P. Chambon, D. Metzger, Spatio-temporally controlled site-specific somatic mutagenesis in the mouse, Proc. Natl. Acad. Sci. USA 94 (1997) 14559–14563.
[44] R. Feil, J. Brocard, B. Mascrez, M. LeMeur, D. Metzger, P. Chambon, Ligand-activated site-specific recombination in mice, Proc. Natl. Acad. Sci. USA 93 (1996) 10887–10890.
[45] Y. Fujinaga, M. Shimada, K. Okazawa, M. Fukushima, I. Kato, K. Fujinaga, Simultaneous detection and typing of genital human papillomavirus DNA using the polymerase chain reaction, J. Gen. Virol. 72 (1991) 1039–1044.
[46] J. Sambrook, E.F. Fritsch, T. Maniatis, Molecular Cloning, Cold Spring Harbor Laboratory Press, Cold Spring Harbor, NY, 1989.
[47] R. Riley, S. Duensing, T. Brake, K. Münger, P.F. Lambert, J.M. Arbeit, Dissection of Human Papillomavirus E6 and E7 Function in transgenic mouse models of cervical carcinogenesis, Cancer Res. 63 (2003) 4862–4871.
[48] W.K. Whitten, Occurrence of anoestrus in mice caged in groups, J. Endocrinol. 18 (1959) 102–107.
[49] Y. Gavrieli, Y. Sherman, S.A. Ben-Sasson, Identification of programmed cell death in situ via specific labeling of nuclear DNA fragmentation, J. Cell Biol. 119 (1992) 493–501.
[50] G.J. Nuovo, Co-labeling using in situ PCR: a review, J. Histochem. Cytochem. 49 (2001) 1329–1339.
[51] F. Kellendonk, F. Tronche, E. Casanova, K. Anlag, C. Opherk, G. Schutz, Inducible site-specific recombination in the brain, J. Mol. Biol. 285 (1999) 175–182.
[52] F. Schwenk, R. Kuhn, P.O. Angrand, K. Rajewsky, A.F. Stewart, Temporally and spatially regulated somatic mutagenesis in mice, Nucl. Acids Res. 26 (1998) 1427–1432.
[53] M. Tannour-Louet, A. Porteu, S. Vaulont, A. Kahn, M. Vasseur-Cognet, A tamoxifen-inducible chimeric Cre recombinase specifically effective in the fetal and adult mouse liver, Hepatology 35 (2002) 1072–1081.
[54] D. Juric, V. Mahovlić, S. Rajhvajn, A. Ovanin-Rakić, L. Skopljanac-Macina, A. Barisić, I.S. Projić, D. Babić, M. Susa, A. Corusić, S. Oresković, Liquid-based cytology—new possibilities in the diagnosis of cervical lesions, Coll. Antropol. 34 (2010) 19–24.
[55] C. Bergeron, J. Ordi, D. Schmidt, M.J. Trunk, T. Keller, R. Ridder, European CINtec histology study group, conjunctive p16INK4a testing significantly increases accuracy in diagnosing high-grade cervical intraepithelial neoplasia, Am. J. Clin. Pathol. 133 (2010) 395–406.
[56] D. Simoni, M. Tolomeo, Retinoids, apoptosis and cancer, Curr. Pharm. Des. 17 (2001) 1823–1837.
[57] J.O. Funk, S. Waga, J.B. Harry, E. Espling, B. Stillman, D.A. Galloway, Inhibition of CDK activity and PCNA-dependent DNA replication by p21 is blocked by interaction with the HPV-16 E7 oncoprotein, Genes Dev. 11 (1997) 2090–20100.
[58] D.L. Jones, R.M. Alani, K. Münger, The human papillomavirus E7 oncoprotein can uncouple cellular differentiation and proliferation in human keratinocytes by abrogating p21Cip1-mediated inhibition of cdk2, Genes Dev. 11 (1997) 2101–2111.
[59] J.M. Adams, S. Cory, The Bcl-2 protein family: arbiters of cell survival, Science 281 (1998) 1322–1326.
[60] H. Liu, C. Zang, M.H. Fenner, D. Liu, K. Possinger, H.P. Koeffler, E. Elstner, Growth inhibition and apoptosis in human Philadelphia chromosome-positive lymphoblastic leukemia cell lines by treatment with the dual PPARalpha/gamma ligand TZD18, Blood 107 (2006) 3683–3692.
[61] H.C. Liu, G.G. Chen, A.C. Vlantis, G.M. Tse, A.T. Chan, C.A. van Hasselt, Inhibition of apoptosis in human laryngeal cancer cells by E6 and E7 oncoproteins of human papillomavirus 16, J Cell Biochem. 103 (2008) 1125–1143.
[62] S. Haldar, A. Basu, C.M. Croce, Bcl2 is the guardian of microtubule integrity, Cancer Res. 57 (1997) 229–233.
[63] T. Chittenden, E.A. Harrington, R. O'Connor, C. Flemington, R.J. Lutz, G.I. Evan, B.C. Guild, Induction of apoptosis by the Bcl-2 homologue Bak, Nature 374 (1995) 733–736.
[64] V. Graupner, E. Alexander, T. Overkamp, O. Rothfuss, V. De Laurenzi, B.F. Gillissen, P.T. Daniel, K. Schulze-Osthoff, F. Essmann, Differential regulation of the proapoptotic multidomain protein Bak by p53 and p73 at the promoter level, Cell Death Differ. 18 (2011) 1130–1139.
[65] P. Nair, K.M. Nair, P.G. Jayaprakash, M.R. Pillai, Decreased programmed cell death in the uterine cervix associated with high risk human papillomavirus infection, Pathol. Oncol. Res. 5 (1999) 95–103.
[66] A. Aguilar-Lemarroy, P. Gariglio, N.J. Whitaker, S.T. Eichhorst, H. zur Hausen, P.H. Krammer, F. Rösl, Restoration of p53 expression sensitizes human papillomavirus type 16 immortalized human keratinocytes to CD95-mediated apoptosis, Oncogene 21 (2002) 165–175.
[67] A. Aguilar-Lemarroy, S. Kirchhoff, N. Whitaker, P. Gariglio, H. zur Hausen, P.H. Krammer, F. Rösl, Differential sensitivity of human papillomavirus type 16(+) and type 18(+) cervical carcinoma cells to CD95-mediated apoptosis, Int. J. Cancer 93 (2001) 823–831.
[68] O. Chakrabarti, S. Krishna, Molecular interactions of "high risk" human papillomaviruses E6 and E7 oncoproteins: Implications for tumour progression, J. Biosci. 28 (2003) 337–348.
[69] Y. Asadurian, H. Kurilin, H. Lichtig, A. Jackman, P. Gonen, M. Tommasino, I. Zehbe, L. Sherman, Activities of human papillomavirus 16 E6 natural variants in human keratinocytes, J. Med. Virol. 79 (2007) 1751–1760.
[70] M. Scheffner, B.A. Werness, J.M. Huibregtse, A.J. Levine, P.M. Howley, The E6 oncoprotein encoded by human papillomavirus type 16 and 18 promotes the degradation of p53, Cell 63 (1990) 1129–1136.
[71] S.A. Sedman, N.L. Hubbert, W.C. Vass, D.R. Lowy, J.C. Schiller, Mutant p53 can substitute for human papillomavirus type 16 E6 in immortalization of human keratinocytes but does not have E6-associated transactivation or transforming activity, J. Virol. 66 (1992) 4201–4208.
[72] H. Pan, A.E. Griep, Temporally distinct patterns of p53-dependent and p53-independent apoptosis during mouse lens development, Genes Dev. 9 (1995) 2157–2169.
[73] S.S. Magal, A. Jackman, S. Ish-Shalom, L.E. Botzer, P. Gonen, R. Schlegel, L. Sherman, Downregulation of Bax mRNA expression and protein stability by the E6 protein of human papillomavirus 16, J. Gen. Virol. 86 (2005) 611–621.
[74] M. Vogt, K. Butz, S. Dymalla, J. Semzow, F. Hoppe-Seyler, Inhibition of Bax activity is crucial for the antiapoptotic function of the human papillomavirus E6 oncoprotein, Oncogene 25 (2006) 4009–4015.
[75] P.J. Duerksen-Hughes, J. Yang, S.B. Schwartz, HPV 16 E6 blocks TNF-mediated apoptosis in mouse fibroblast LM cells, Virology 264 (1999) 55–65.
[76] M. Filippova, L. Parkhurst, P.J. Duerksen-Hughes, The human papillomavirus 16 E6 protein binds to Fas-associated death domain and protects cells from Fas-triggered apoptosis, J. Biol. Chem. 279 (2004) 25729–25744.
[77] H. Yuan, F. Fu, J. Zhuo, W. Wang, J. Nishitani, D.S. An, I.S. Chen, X. Liu, Human papillomavirus type 16 E6 and E7 oncoproteins upregulate c-IAP2 gene expression and confer resistance to apoptosis, Oncogene 24 (2005) 5069–5078.
[78] M. Branca, M. Ciotti, C. Giorgi, D. Santini, L. Di Bonito, S. Costa, A. Benedetto, D. Bonifacio, P. Di Bonito, P. Paba, L. Accardi, S. Syrjänen, C. Favalli, K. Syrjänen, HPV-PathogenISS Study Group, Up-regulation of proliferating cell nuclear antigen (PCNA) is closely associated with high-risk human papillomavirus (HPV) and progression of cervical intraepithelial neoplasia (CIN), but does not predict disease outcome in cervical cancer, Eur. J. Obstet. Gynecol. Reprod. Biol. 130 (2007) 223–231.
[79] P. Samarawardana, D.L. Dehn, M. Singh, D. Franquemont, C. Thompson, L. Gaido, K.C. Torkko, P. Homer, S. Burke, M.A. Titmus, V. Nayi, K.R. Shroyer, p16(INK4a) is superior to high-risk human papillomavirus testing in cervical cytology for the prediction of underlying high-grade dysplasia, Cancer Cytopathol. 118 (2010) 146–156.
[80] H.S. Zhang, A.A. Postigo, D.C. Dean, Active transcriptional repression by the Rb-E2F complex mediates G1 arrest triggered by p16INK4a, TGFbeta, and contact inhibition, Cell 97 (1999) 53–61.
[81] M.E. McLaughlin-Drubin, K.W. Huh, K. Münger, Human papillomavirus type 16 E7 oncoprotein associates with E2F6, J. Virol. 82 (2008) 8695–8705.
[82] M.E. McLaughlin-Drubin, C.P. Crum, K. Münger, Human papillomavirus E7 oncoprotein induces KDM6A and KDM6B histone demethylase expression and causes epigenetic reprogramming, Proc. Natl. Acad. Sci. USA 108 (2011) 2130–2135.
[83] J.M. Trimarchi, B. Fairchild, J. Wen, J.A. Lees, The E2F6 transcription factor is a component of the mammalian Bmi1-containing polycomb complex, Proc. Natl. Acad. Sci. USA 98 (2001) 1519–1524.
[84] R.H. Kim, M.K. Kang, K.H. Shin, Z.M. Oo, T. Han, M.A. Baluda, N.H. Park, Bmi-1 cooperates with human papillomavirus type 16 E6 to immortalize normal human oral keratinocytes, Exp. Cell Res. 313 (2007) 462–472.
[85] H.Y. Lee, D.F. Dohi, Y.H. Kim, G.L. Walsh, U. Consoli, M. Andreeff, M.I. Dawson, W.K. Hong, J.M. Kurie, All-trans retinoic acid converts E2F into a transcriptional suppressor and inhibits the growth of normal human bronchial epithelial cells through a retinoic acid receptor- dependent signaling pathway, J. Clin. Invest. 101 (1998) 1012–1019.
[86] T.A. Baudino, K.H. Maclean, J. Brennan, E. Parganas, C. Yang, A. Aslanian, J.A. Lees, C.J. Sherr, M.F. Roussel, J.L. Cleveland, Myc-mediated proliferation and lymphomagenesis, but not apoptosis, are compromised by E2f1 loss, Mol. Cell. 11 (2003) 905–914.
[87] S. Pelengaris, M. Khan, The many faces of c-MYC, Arch. Biochem. Biophys. 416 (2003) 129–136.
[88] J. Secombe, S.B. Pierce, R.N. Eisenman, Myc: a weapon of mass destruction, Cell 117 (2004) 153–156.
[89] K.A. O'Donnell, E.A. Wentzel, K.I. Zeller, C.V. Dang, J.T. Mendell, c-Myc-regulated microRNAs modulate E2F1 expression, Nature 435 (2005) 839–843.
[90] W.S. el-Deiry, T. Tokino, V.E. Velculescu, D.B. Levy, R. Parsons, J.M. Trent, D. Lin, W.E. Mercer, K.W. Kinzler, B. Vogelstein, WAF1, a potential mediator of p53 tumor suppression, Cell 75 (1993) 817–825.
[91] R. Li, S. Waga, G.J. Hannon, D. Beach, B. Stillman, Differential effects by the p21 CDK inhibitor on PCNA-dependent DNA replication and repair, Nature 371 (1994) 534–537.
[92] S. Balsitis, F. Dick, D. Lee, L. Farrell, R.K. Hyde, A.E. Griep, N. Dyson, P.F. Lambert, Examination of the pRb-dependent and pRb-independent functions of E7 in vivo, J. Virol. 79 (2005) 11392–11402.